Positron mobility in Si at 300 K

J. Mäkinen, C. Corbel,* P. Hautojärvi, and A. Vehanen
Laboratory of Physics, Helsinki University of Technology, 02150 Espoo, Finland

D. Mathiot
Centre National d'Etudes des Télécommunications, Boîte Postale 98, 38243 Meylan, France
(Received 4 December 1989)

Positron motion in an electric field is studied experimentally by measuring the drift length of positrons in the space-charge region of a Au-Si surface-barrier diode. An electric field of the order of 10^4 V/cm gives rise to a drift length from 2 to 3 μm. The drift-diffusion approximation can explain positron transport up to an electric-field strength of 3×10^4 V/cm. At 300 K we get a positron mobility of 120 ± 10 cm^2/V s in Czochralski-grown Si ($[P]=7.4\times10^{14}$ cm^{-3}), and the diffusion coefficient calculated from the Einstein relation is 3.0 ± 0.25 cm^2/s. Positron diffusion was measured without preparing a metal-semiconductor contact in high-purity floating-zone Si (10^4 Ω cm) assuming the electric field can be neglected. The diffusion coefficient is 3.10 ± 0.20 cm^2/s, in good agreement with that based upon the positron mobility measured under an electric field.

I. INTRODUCTION

The motion of positrons in solids is of interest as a measure of positron-interaction processes. Motion of thermal positrons is diffusive, limited predominantly by scattering from lattice vibrations. Positron motion is of interest also in different kinds of experiments, such as positron trapping at lattice defects or momentum-density measurements. Positron annihilation in near-surface layers and thin films is increasingly studied following the progress in the production of low-energy positron beams.[1] Those experiments are in many cases directly involved with positron diffusion to the surface.

Recently, an extensive study of positron diffusion in a number of cubic metals was reported by Soininen *et al.*[2] Positron motion was shown to be limited by acoustic-phonon scattering in a wide temperature region from 20 K to the onset of positron trapping at thermal vacancies, and at 300 K the diffusion coefficient is $1-2$ cm^2/s.

In semiconductors the influence of electric fields on positron motion needs to be considered. The study of positron motion in semiconductors began with the drift-velocity measurements of Mills and Pfeiffer[3,4] in Ge and Si γ-ray detectors. The drift velocities of electrons and holes in Si and Ge have been determined using the time-of-flight technique.[5-8] The carrier transport is understood in terms of weak scattering from optical and acoustic phonons. Positrons exhibit transport behavior similar to that of electrons and holes. The lattice-scattering mechanisms for positrons are predominantly due to phonon scattering, but coupling to the lattice is stronger than for the charge carriers, implying a higher effective mass and consequently a lower mobility. The positron can be viewed as another charge carrier, with a simple band structure in elemental semiconductors and with a wide range of temperatures attainable for the measurement of transport properties.

There are relatively few studies of positron motion in semiconductors making use of low-energy positron beams, and the results are in many cases diverse. In Si and Ge the reported positron diffusion coefficients vary significantly, showing unexpected dependence on temperature, doping, and heat treatments.[9-12] This has been partly ascribed to the fact that in semiconductors the positron motion is subject to electric fields in the space-charge region at the surface. Uenodo *et al.*[13] have reported results showing that positron annihilation characteristics change with the bias voltage applied to a Si-SiO_2-Si structure. However, the electric field has been unknown in most experiments, and its effect has been ignored.

Recently, Simpson *et al.*[14] published a measurement of positron mobility in Si using the positron-lifetime technique. Their work was based on the drift of positrons to a Au-Si interface, after implantation from a ^{22}Na source to Si through the Au overlayer, and monitoring the lifetime spectra. At 300 K they find the positron mobility 100 ± 18 cm^2/V s.

In this paper we present results of a study of positron motion under the influence of the electric field in the space-charge region of a metal-semiconductor contact. Positrons are implanted through a thin Au overlayer to n-type Si, and after reaching thermal energies they are drifted to the Au-Si interface. The influence of electric field on positron motion in the space-charge region of a surface-barrier diode is demonstrated. When positron motion is described within the drift-diffusion approximation, the Ohmic mobility of 120 ± 20 cm^2/V s and the positron diffusion coefficient 3.0 ± 0.25 cm^2/s at 300 K are determined. We also measured positron diffusion without preparing a metal-semiconductor contact in a high-purity floating-zone (FZ) Si sample, where the drift length is assumed to be much less than the diffusion length because of the small electric field. Some of the ex-

 ©1990 The American Physical Society

perimental results have been published earlier.[15]

The principle of measuring positron diffusion using low-energy positrons is outlined in Sec. II. In Sec. III the experimental details are given, and the results are presented in Sec. IV. In Sec. V the positron mobility resulting from the fitting of the drift-diffusion model to the experimental data is given. In Sec. VI results are compared with previous experiments and the scattering mechanisms are briefly discussed.

II. MEASUREMENT OF POSITRON MOBILITY: PRINCIPLE OF THE METHOD

Measurement of positron diffusion making use of low-energy positron beams has been recently discussed in detail by Schultz and Lynn[1] and Huomo *et al.*[16] When applied to metals, this technique has been shown to give consistent results on the positron diffusion in the temperature range 20–1400 K.[2] We apply the same method to semiconductors, with the difference that the electric-field effects are included. The experimental technique relies on the measurement of the fraction of positrons that, after implantation to silicon through a thin Au overlayer, returns to the Au-Si interface under the influence of an applied electric field. The electric-field strength in the space-charge region of the metal-semiconductor contact is varied by applying an external bias voltage to the Au-Si surface-barrier diode. In the experiment a low-energy positron beam having an incident energy of 0–30 keV was made to strike the sample. After implantation positrons rapidly reach thermal energies, and thermalization is followed by free diffusion in the lattice. The annihilation characteristics differ between positrons returning to the interface or to the surface and those annihilating in the bulk Si. Consequently it becomes possible to distinguish between the two, e.g., by measuring the shape of the 511-keV annihilation line.

Positron thermalization before annihilation is reasonably well established in metals, and positrons are known to reach thermal equilibrium in the lattice well within their lifetime down to temperatures $T<25$ K.[17,18] There is no direct information on positron thermalization in semiconductors, even though Shulman *et al.*[19] have reported evidence of positron thermalization in Ge below 80 K. Unlike in metals, excitation of electron-hole pairs does not occur at the positron kinetic energies less than the band gap, and the final stage of slowing down is due to positron-phonon scattering. However, phonon scattering takes over as the most effective energy-loss mechanism also in metals when the positron energy is around 1 eV, and therefore the thermalization times are not very different in metals and semiconductors. Positrons are expected to reach thermal energies at 300 K in a time which is short (<10 ps) compared with the lifetime of 220 ps in Si.

The 511-keV annihilation line shows Doppler broadening originating from the momentum distribution of the annihilating electron-positron pairs. The line shape is described by the parameter *S*, defined as the relative area of a fixed central region of the 511-keV line. Each positron state yields a distinct value of *S*, and the line-shape parameter is linearly weighted by the fractions of positrons annihilating at different states. In terms of the fraction J of positrons returning to the Au-Si interface before annihilation, the line-shape parameter is

$$S(E,V_b)=J(E,V_b)S_i+[1-J(E,V_b)]S_b \; . \quad (1)$$

In Eq. (1), S_b and S_i are the line-shape parameters characteristic of positron annihilation in Si and positrons reaching the interface and annihilating there. The probability of positron returning to the interface is a function of both the incident positron energy E and the applied bias voltage V_b. All positrons can be made to annihilate either in Si or in the interface region simply by adjusting the incident positron energy and the electric-field strength. This makes a direct measurement of the characteristic line-shape parameters S_b and S_i possible.

The measurement of the line-shape parameter only gives the integral probability that a positron will return to the interface before annihilation. To find the positron mobility, positron transport is described using the drift-diffusion approximation familiar from the classical carrier transport models. Knowledge of the positron stopping profile enables one to deduce the positron mobility and the diffusion coefficient. The main sources of error come from the different parameters inherent in the positron stopping profile and the electric field. These are discussed in Sec. V. Positron trapping at vacancy defects or at low temperatures also at negatively charged impurities[20,21] strongly reduces the drift length, and would lead to a wrong interpretation of the positron mobility or the diffusion coefficient. This is of concern especially in semiconductors exhibiting extremely high positron trapping rates at low temperatures.[22] However, positron trapping can be neglected here. The samples were of *n*-type Si in which there are no as-grown defects that trap positrons, and the concentration of negatively charged impurities is presumably too small to cause any trapping at 300 K.

III. EXPERIMENTAL DETAILS

A. Samples

The Schottky-barrier diodes were prepared on phosphorus doped *n*-type Si crystals cut from a Czochralski-grown wafer. The Au-Si interface was fabricated by evaporating a 100 Å Au layer through an 8-mm-diam mask onto the Si crystal. Diodes of 1 mm diameter were also prepared for current and capacitance measurements.

The carrier concentration in Si and the height of the surface barrier were determined from the 1-mm-diam diodes. From the capacitance-voltage measurement we find the carrier concentration 7.4×10^{14} cm^{-3} and the barrier height 0.83 eV, in good agreement with the barrier height typically reported for contacts formed by Au and *n*-type Si.[23] The current-voltage characteristics of the 1-mm-diam contacts showed the typical diode behavior with the reverse current less than 0.1 μA.

The contact to the backside of the *n*-type Si crystal was made by deposition of metallic gallium. The current-voltage characteristics of the 8-mm diam diode were measured *in situ* when the diode was mounted to the sample holder in ultrahigh vacuum. The current-voltage behav-

ior is shown in Fig. 1. The reverse current is less than 10 μA for the reverse bias voltage $|V_b| < 5$ V. When a forward bias voltage is applied the current increases exponentially up to 150 mV. At higher forward bias voltages, however, the increase of the current is clearly reduced. This is attributed to the series resistance in the contact in the backside of the Si crystal. The current-voltage curve is very well reproduced assuming a series resistance of 1.4 kΩ, and in the case of forward bias the voltage in the space-charge region of the Au-Si contact was corrected for the voltage drop in the series resistance.

The high-purity Si sample was cut from a floating zone-refined silicon ingot. The resistivity of this material was 10^4 Ω cm. The residual boron and phosphorus concentrations based on photoluminescence measurements were 3.3×10^{12} and 1.4×10^{12} cm^{-3}, respectively. The oxygen and carbon contents were below the detection limit of 10^{15} cm^{-3}. The sample surface was etched before mounting to the UHV chamber.

B. Positron beam

The measurements were performed with the low-energy positron beam described in detail in Ref. 24. The sample was mounted to the sample holder in an ultrahigh vacuum chamber, and a monoenergetic ($\Delta E \leq 3$ eV) positron beam having a diameter of 4 mm and an intensity of 10^6 e^+/s was made to strike the sample. The incident positron energy was varied from 0.1 to 28 keV. The 511-keV annihilation line was recorded with a high-purity Ge detector, and the spectra were acquired with a digitally stabilized MCA system. The full width at half maximum (FWHM) of the annihilation line was 3.2 keV when all positrons annihilate in Si, and the central region of the peak defining the line-shape parameter S was taken to be 1.8 keV. The detector was mounted perpendicular to the electric-field direction so that the Doppler shift of the annihilation peak can be neglected. At each incident energy and applied electric field, 10^6 counts were collected to the 511-keV annihilation line. The resolution measured with a ^{207}Bi source (570 keV) was 1.50 keV (FWHM).

IV. RESULTS

Figure 2 presents the line-shape parameter S measured as a function of the incident positron energy $E = 0.1-28$ keV for different applied bias voltages. The bias voltage applied to the Au-Si contact varies from $+0.18$ V (forward bias) to -4.0 V (reverse bias). For all bias voltages the electric field in the space-charge region in Si is directed towards the Au-Si interface, causing an enhanced transport of positrons to the interface. The field strength increases as the applied bias voltage becomes more negative.

At low incident energies $E < 2.5$ keV, positron annihilation is independent of the applied bias voltage. In this energy range positrons are implanted into the 100 Å Au overlayer, and annihilation takes place in the Au layer or at the Au-Si interface. Positrons may also escape from the surface. Due to the incident energy of only a few keV, all positrons do not have time to reach thermal en-

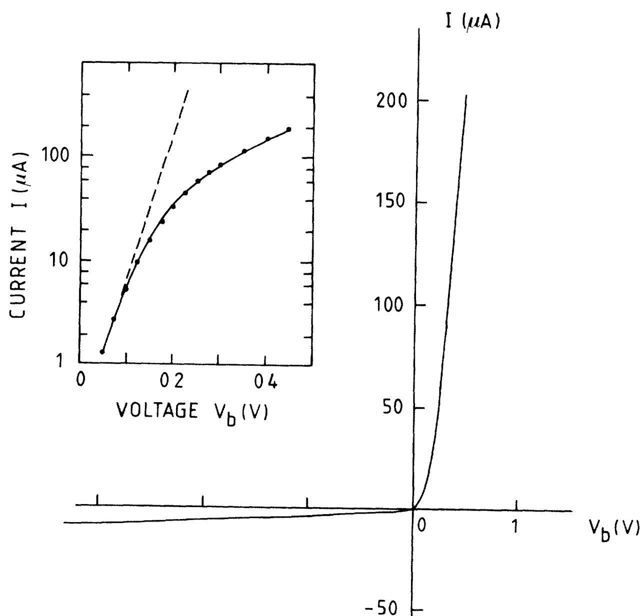

FIG. 1. The current-voltage characteristics of the Au-Si Schottky-barrier diode measured *in situ* with the diode mounted to the sample holder in ultrahigh vacuum. The inset shows the forward current, and the solid line in the inset is calculated assuming a series resistance of 1.4 kΩ.

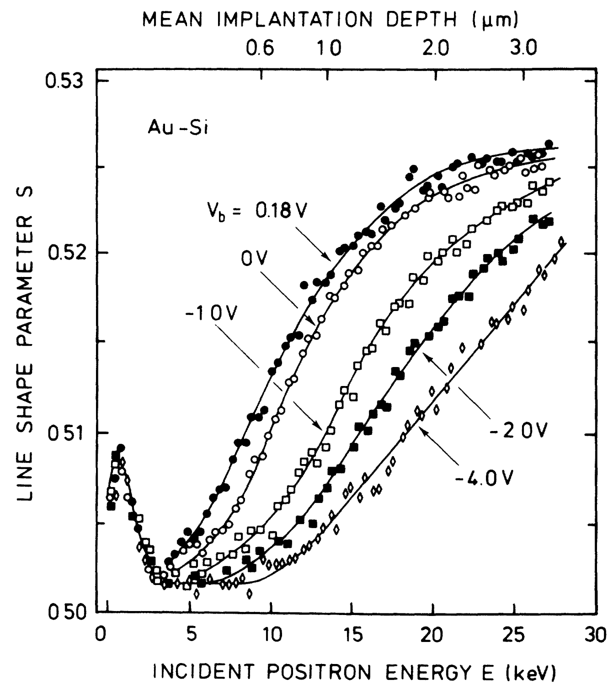

FIG. 2. The line-shape parameter S as a function of the incident positron energy at applied bias voltages from $V_b = +0.18$ (forward bias) to -4.0 V (reverse bias). The mean implantation depth, given for incident energies $E \geq 9$ keV, represents the stopping profile in Si. The solid lines are guides for the eye only.

ergies before they return to the surface, and these epithermal positrons strongly affect the annihilation characteristics. At higher incident positron energies $E > 2.5$ keV the fraction of positrons implanted into the Au layer rapidly decreases and positrons penetrate through the overlayer to silicon. At 10 keV the fraction of positrons stopped in the Au layer is approximately 1%, and at higher incident energies the Au overlayer becomes fully transparent to positrons. Clearly, as positrons are implanted to silicon, the line-shape parameter becomes strongly dependent on the applied bias voltage.

The experimental data in Fig. 2 indicates that positrons reaching the Au-Si interface and annihilating there yield a well-defined value S_i for the line-shape parameter. In particular, at the applied bias voltage $V_b = -4.0$ V the electric-field strength is sufficiently high to drift all the positrons to the interface prior to annihilation at the incident positron energies $E \leq 9$ keV. This is observed as a constant value of S. The same tendency with a common value of S at the interface is observed also at lower bias voltages. No positron or positronium emission into vacuum from the sample surface was detected at the incident positron energies above 2 keV.

At high incident positron energies $E > 25$ keV, the number of positrons returning to the interface region finally vanishes. Extrapolating from the $V_b = +0.18$ or 0.0 V data in Fig. 2, we find the characteristic value of $S_b = 0.5272 \pm 0.0002$ for free positron annihilation in Si.

In Fig. 2 the change in the line-shape parameter $S(E, V_b)$ at different applied bias voltages indicates that the probability that a positron returns to the Au-Si interface is strongly enhanced as the reverse bias voltage increases. This is observed as a smaller value of the line-shape parameter resulting from an increasing fraction of positrons drifted to the interface before annihilation. The value of S equal to $(S_i + S_b)/2$ represents the condition in which half of the positrons are drifted to the Au-Si interface. This occurs at the incident energy of 10 keV when the applied bias voltage is $V_b = +0.18$ V, and at 23 keV when the reverse bias is $V_b = -4.0$ V. The mean implantation depth for 23 keV incident positrons in Si is approximately 2.9 μm. The average electric field in the space-charge region corresponding to $V_b = -4.0$ V is 1.6×10^4 V/cm, and the width of this region is 2.8 μm (see Sec. V). This field is able to drift positrons over about 2–3 μm during their lifetime of 220 ps. These numbers give an order-of-magnitude estimate for the positron mobility $\mu_+ = 100$ cm^2/V s at 300 K.

Figure 3 presents the line-shape parameter S as a function of the applied bias voltage $V_b = +0.15$ to -4.0 V measured at constant incident positron energies $E = 7.5$, 10.0, 15.0, and 20.0 keV. The influence of the electric field is obvious also here. As the applied reverse bias increases, the value of S decreases because of a higher fraction of positrons drifted to the interface. At the incident positron energy 7.5 keV, the line-shape parameter reaches a constant value when the reverse bias voltage is $V_b < -1.5$ V, and the lowest measured values of S are from 0.5010 to 0.5015. This is taken as the characteristic value S_i for positrons annihilating after they have reached the Au-Si interface.

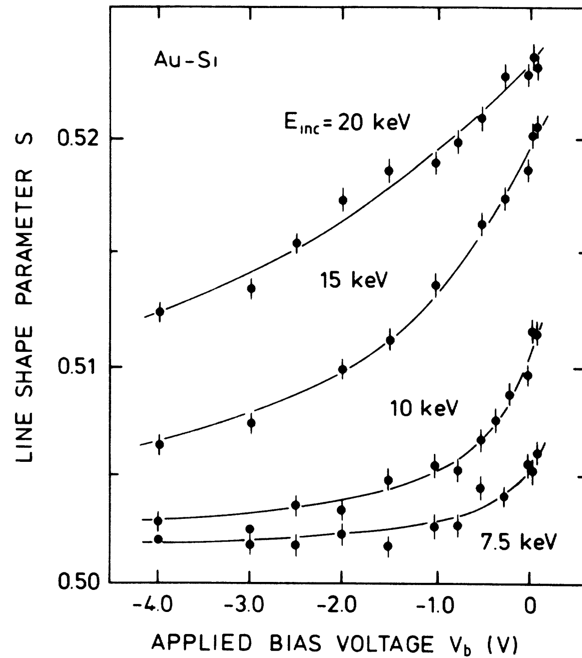

FIG. 3. The line-shape parameter S as a function of the applied bias voltage for incident positron energies $E = 7.5$, 10.0, 15.0, and 20 keV. The solid lines are least-squares fits to the drift-diffusion model corresponding to the positron mobilities $\mu_+ = 125$, 117, 108, and 110 cm^2/V s, respectively.

The electric field corresponding to the applied forward bias voltage $V_b = +0.18$ V is sufficient to significantly affect the positron motion. If higher forward bias voltages are applied, the voltage drop in the series resistance induced by increasing current across the junction cancels the increase in V_b to a large extent (see Fig. 1). In consequence, the electric field in the space-charge region of the Au-Si contact remains nearly unchanged and lower electric fields are unattainable. This is also observed in the line-shape parameter, which becomes independent of the applied bias voltage.

Positron diffusion was measured also in the 10^4 Ω cm FZ Si sample, and the line-shape parameter $S(E)$ is shown in Fig. 4. As a function of the incident positron energy the line-shape parameter is qualitatively similar to those measured at zero or forward bias voltages in the Au-Si surface-barrier diode (Fig. 2) except that there is a shift in the energy due to the absence of the Au overlayer. The incident energy corresponding to the condition in which half of the positrons return to the surface before annihilation is approximately 5 keV. Comparing Figs. 2 and 4, the line-shape parameter in the FZ Si sample reaches a level close to that of bulk Si at smaller positron implantation depths, indicating a shorter drift length than in the surface-barrier diode at $V_b = +0.18$ V. Although the exact electric field in the FZ Si sample is not known, it is estimated that, owing to the low concentration of charged impurities, the field is much less than 1 keV/cm. Consequently, the drift length is much shorter than the diffusion length, and we consider the influence of the field on positron motion to be small.

Figures 2 and 3 demonstrate the influence of the elec-

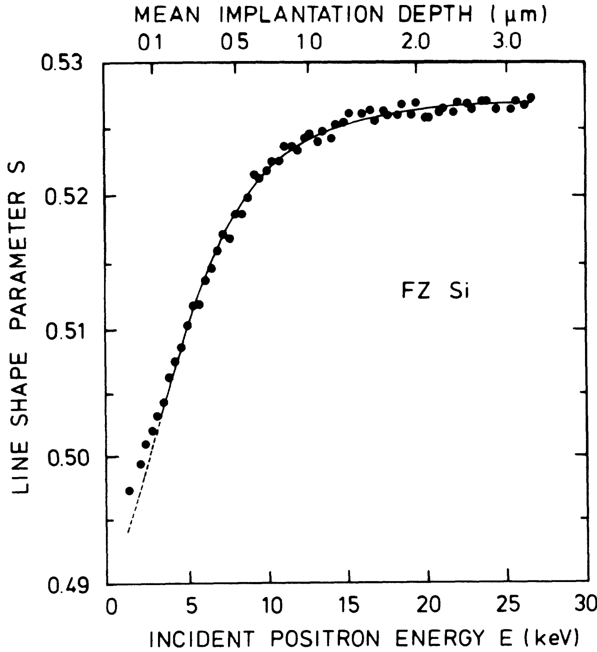

FIG. 4. The line-shape parameter S as a function of the incident positron energy measured in the floating-zone Si sample at 300 K. The solid line is a least-squares fit to the diffusion model with $D_+ = 3.10 \pm 0.20$ cm^2/s assuming there is no electric field.

tric field on positron motion. In Sec. V the drift-diffusion approximation is used to describe positron transport and to find the positron mobility and the diffusion coefficient at 300 K.

V. POSITRON MOBILITY

A. Drift-diffusion model

A simple, yet fairly successful, way of describing positron motion in solids starts from the diffusion equation.[1,25] In the following we have modeled positron transport using the drift-diffusion approximation familiar from the classical carrier transport models. This requires the solution of the continuity equation

$$\frac{\partial n_+(\mathbf{r},t)}{\partial t} = -\nabla\cdot[n_+(\mathbf{r},t)\mathbf{v}_+] - \lambda n_+(\mathbf{r},t) \ , \qquad (2)$$

where $n_+(\mathbf{r},t)$ is the distribution of thermal positrons, λ is the annihilation rate, and $\mathbf{v}_+$ is the positron velocity

$$\mathbf{v}_+ = \mathbf{v}_d - \frac{D_+}{n_+(\mathbf{r},t)}\nabla n_+(\mathbf{r},t) \ . \qquad (3)$$

Here $\mathbf{v}_d$ and D_+ are the positron drift velocity and the diffusion coefficient. From Eqs. (2) and (3) the quasistationary drift-diffusion equation follows:

$$D_+\nabla^2 n_+(\mathbf{r}) - \lambda n_+(\mathbf{r}) - \nabla\cdot[n_+(\mathbf{r})\mathbf{v}_d] + P_E(\mathbf{r}) = 0 \ . \qquad (4)$$

In Eq. (4) $P_E(\mathbf{r})$ is the positron stopping profile, or more rigorously the introduction rate of positrons, which represents the initial distribution $n_+(\mathbf{r},t=0)$ in Eqs. (2) and (3). This model, assuming diffusive motion, is limited to positrons implanted at depths of several scattering mean free paths, and is expected to be valid except at very low incident positron energies or sample temperatures.[25] The mean free path for positron scattering at 300 K is typically only a few nanometers,[17,26] whereas in the experiment positrons are drifted over distances which are much longer.

The electric field $\mathcal{E}$ in the space-charge region of the metal-semiconductor contact is calculated in the depletion layer approximation (see, e.g., Ref. 27)

$$\mathcal{E}(x) = \frac{qN_D}{\epsilon_s}(W - x) \ . \qquad (5)$$

The field is directed towards the Au-Si interface, x denoting the distance from the interface. The width W of the depletion region is

$$W = \left[\frac{2\epsilon_s}{qN_D}\left[V_{\text{bi}} - V_b - \frac{k_B T}{q}\right]\right]^{1/2} \ . \qquad (6)$$

Above, N_D is the donor concentration in the space-charge region, ϵ_s is the dielectric constant, V_b is the external bias voltage, and qV_{bi} is the diffusion potential

$$qV_{\text{bi}} = \phi_b - (E_C - E_F) \ , \qquad (7)$$

where ϕ_b is the Schottky-barrier height and $E_C - E_F$ is the Fermi-level position measured from the bottom of the conduction band. In this standard approximation the electric field has its maximum value at the interface, and the field decreases linearly to zero at the end of the depletion region.

The stopping profile of keV positrons is taken as

$$P_E(x) = -\frac{d}{dx}\exp\left[-\left[\frac{x-\delta}{x_0}\right]^m\right] \ , \qquad (8)$$

where

$$x_0 = (\alpha/\rho)(E/\text{keV})^n \ . \qquad (9)$$

The stopping profile (8) is based on Monte Carlo simulations of positron slowing down[28] and experimental studies of multilayer structures.[29] Those studies also yield the parameters $m = 1.9-2.0$, $n = 1.5-1.6$, and $\alpha = 4.5$ μg/cm^2 nearly independent of the target material. In the Au-Si structure studied here, the stopping profile in silicon was determined simply by requiring the positron transmission to be continuous. Effectively, the 100 Å Au layer is replaced with a Si layer of equal mass per unit area, and this condition determines the parameter $\delta = -(\rho_{\text{Au}}/\rho_{\text{Si}})\Delta_{\text{Au}}$ where Δ_{Au} is the Au-layer thickness. In this approximation the difference in backscattering is neglected, and the stopping profile parameters are taken independent of the atomic number. The positron implantation depth is almost entirely determined by the inelastic collisions with electrons in the early stages of slowing down, and the electric field is not expected to distort the stopping profile.

In the linear-response regime the drift velocity $\mathbf{v}_d$ depends on the electric field through the field-independent mobility μ_+ as

$$v_d = \mu_+ \mathcal{E} \ . \qquad (10)$$

For Eq. (10) to be valid, the drift velocity should be small compared with the thermal-equilibrium velocity. The maximum electric field for the highest applied reverse bias voltage $V_b = -4.0$ V is approximately 3×10^4 V/cm. Assuming the positron mobility is of the order of 100 cm^2/V s, as estimated in the preceding section, the drift velocity is always less than 3×10^6 cm/s. The thermal positron velocity is 1.1×10^7 cm/s at 300 K, and we make the approximation (10) at the relatively high electric fields assuming the positron mobility to be field independent. The fact that the drift velocity is small compared to the thermal-equilibrium velocity is a prerequisite also for the diffusion model to be valid.

In principle, the positron mobility and the diffusion coefficient could be determined independently. However, the diffusion term in Eq. (4) is significantly smaller than the drift term at the applied bias voltages $V_b = +0.18$ to -4.0 V. The fact that the drift length $l_+ = v_d \tau$ is always much longer than the diffusion length makes an independent determination of D_+ overly uncertain. Therefore, the diffusion coefficient was expressed in terms of the mobility by means of the Einstein relation

$$D_+ = \frac{k_B T}{q} \mu_+ \ . \qquad (11)$$

Assuming the interface to be abrupt, the boundary condition for the positron density at the Au-Si interface is

$$J = D_+ \frac{dn_+}{dx}\bigg|_{x=0} + v_d n_+(x=0) = \nu n_+(x=0) \ . \qquad (12)$$

This simply states that the positron flux must be equal to the rate of disappearance at the interface. The transition rate ν includes both the positron escape to the Au layer and possible trapping at the interface region. The left-hand side of Eq. (12) also gives the fraction J of positrons returning to the interface.

The drift-diffusion equation (4) was transformed to a system of first-order equations and solved numerically in one dimension to find the positron density and the number of positrons drifted to the interface before annihilation. The values for different parameters appearing in Eqs. (4)–(12) are given in Sec. V B.

B. Positron mobility

To deduce the positron mobility and the diffusion coefficient, least-squares fits of the drift-diffusion model to the measured line-shape parameter $S(E,V_b)$ were carried out. In Eq. (1), $J(E,V_b)$ was solved from Eqs. (4)–(12) and the characteristic line-shape parameters $S_i = 0.5010$ and $S_b = 0.5272$ were given the experimental values. We have also used Eq. (1) and the experimental values of $S(E)$ in Fig. 2 to calculate the fraction of positrons returning to the interface before annihilation at different bias voltages. Figure 5 shows $J(E,V_b)$ for the incident positron energies $E \geq 9$ keV.

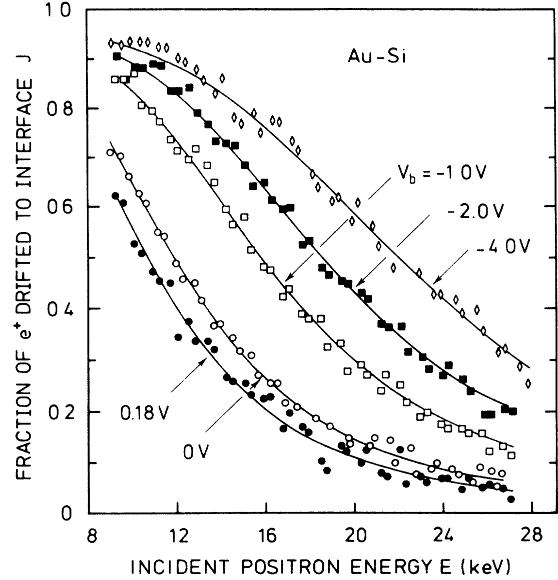

FIG. 5. The fraction of positrons entering the interface before annihilation calculated from Eq. (1) and the line-shape parameter $S(E)$ in Fig. 2. The solid lines are least-squares fits to the drift-diffusion model assuming a field-independent positron mobility. The resulting values of μ_+ are given in Table II.

The solid lines in Figs. 3 and 5 are least-squares fits to the drift-diffusion model. The values of the parameters in Eqs. (4)–(12) are listed in Table I. For the carrier concentration and the surface-barrier height we use the values 7.4×10^{14} cm^{-3} and 0.83 eV based on the capacitance-voltage measurements. The carrier concentration also yields the Fermi-level position $E_C - E_F = 0.273$ eV in Si at 300 K, determining the diffusion potential in Eq. (7). Positron annihilation rate is $\lambda = 1/\tau$, where $\tau = 220$ ps is the free positron lifetime in Si.[30] The transition rate at the interface is taken as $\nu = \infty$, i.e., the interface is assumed to be totally absorbing implying a vanishing positron density at the interface.

TABLE I. The values of parameters in the drift-diffusion model, Eqs. (4)–(12).

Density	ρ_{Si}	2.33 g/cm^3
	ρ_{Au}	19.3 g/cm^3
Dielectric constant of Si	ϵ_s	11.9
Donor concentration	N_D	7.4×10^{14} cm^{-3}
Au-layer thickness	Δ_{Au}	100 Å
Schottky-barrier height	ϕ_b	0.83 eV
Fermi-level position	$E_C - E_F$	0.273 eV
Positron stopping profile	m	2.0
	n	1.60
	α	4.50 μg/cm^2
Positron annihilation rate	λ	4.54×10^9 s^{-1}
Surface transition rate	ν	∞
Line-shape parameter	S_i	0.5010
	S_b	0.5272

The positron mobility turned out to be strongly affected by the stopping profile parameters n and α, which determine the positron implantation depth. To extract their values two different methods were used. If the line-shape parameters S_i and S_b are considered as free parameters, they both reach a common value $S_i=0.5010-0.5015$ and $S_b=0.5272-0.5276$ when $n=1.60-1.62$ and $\alpha=4.50$ μg/cm^2, independent of the applied bias voltage. We also carried out an analysis keeping both n and μ_+ variables. Such analysis yields $n=1.60\pm0.01$. These values of n and α very well agree with the stopping profile parameters reported earlier,[28,29] and thus they were fixed to the values $n=1.60$ and $\alpha=4.50$ μg/cm^2. The incident positron energies $E<9$ keV were omitted to exclude the effects of epithermal positrons and uncertainties in the stopping profile close to the interface.

The values for the positron mobility resulting from the least-squares fits to the line-shape parameter $S(E,V_b)$ in Fig. 5 are given in Table II. The maximum electric fields together with the widths of the depletion region for each applied bias voltage are also given. At applied bias voltages from $V_b=+0.18$ to -4.0 V the mobility at 300 K varies from 115 to 125 cm^2/V s. These values are within the estimated error $\sigma_\mu=10$ cm^2/V s. The line-shape parameter S in Fig. 3 measured at constant incident positron energies was fitted in a similar way. The mobilities corresponding to the incident energies of 7.5, 10.0, 15.0, and 20.0 keV are 125, 117, 108, and 110 cm^2/V s, respectively. These values are equal to those given in Table II within the estimated error, and we consider that they correspond to a mobility of 120 ± 10 cm^2/V s. The Einstein relation then gives the diffusion coefficient $D_+=3.0\pm0.25$ cm^2/s.

We have also estimated the importance of different parameters listed in Table I contributing to uncertainties in the positron mobility. If S_i is changed from 0.5010 to 0.5015, positron mobility increases approximately 10 cm^2/V s independent of the applied bias voltage. The Schottky-barrier height has influence on the mobility only when the applied bias voltage is small. At the applied bias voltages $V_b=-2.0$ or -4.0 V, a change of 0.1 V in the barrier height ϕ_B causes a change $\Delta\mu_+<5$ cm^2/V s in positron mobility. A 40 Å change in the nominal Au-layer thickness changes the mobility approximately 15 cm^2/V s when the bias voltage is $V_b=0.0$ V and less than 5 cm^2/V s when $V_b=-4.0$ V.

TABLE II. The maximum electric field $\mathcal{E}_{max}$ and the width of the depletion region W for different applied bias voltages V_b calculated from Eqs. (5) and (6). The values of positron mobility are from the fits to the drift-diffusion model presented in Fig. 5 assuming μ_+ to be independent of the electric-field strength. The diffusion coefficient is calculated from the Einstein relation $D_+=(k_BT/q)\mu_+$.

V_b (V)	$\mathcal{E}_{max}$ (kV/cm)	W (μm)	μ_+ (cm^2/V s)	D_+ (cm^2/s)
+0.18	8.9	0.791	120	3.05
0	10.9	0.972	121	3.05
−1.00	18.5	1.650	115	2.90
−2.00	23.8	2.121	125	3.15
−4.00	31.9	2.838	123	3.10

In conclusion, including the uncertainties in different parameters we estimate the positron mobility in Si to be $\mu_+=120\pm20$ cm^2/V s at 300 K.

The line-shape parameter $S(E)$ measured from the FZ Si sample was analyzed assuming a zero electric field. The positron stopping profile was the same, except that $\delta=0$ in Eq. (8). We consider only the line-shape parameter measured at incident positron energies $E>3.0$ keV whereafter the analysis is independent of the minimum energy included. The deviation from the experimental values at smaller incident energies in Fig. 4 is attributed to epithermal positron emission.[31] The resulting positron diffusion constant is $D_+=3.10\pm0.20$ cm^2/s, and the energy E_0 (see Sec. VI) correspondingly 5.10 ± 0.10 keV.

VI. DISCUSSION AND CONCLUSIONS

There exists relatively few published studies of positron motion in semiconductors, and the results are often obscured because of the unknown electric fields. The electric field in the space-charge region of the Au-Si surface-barrier diode studied here is known to a good approximation. Under the influence of the applied electric field of the order for 10^4 kV/cm positrons are drifted a few μm during their lifetime of 220 ps. The drift term becomes significant when the drift length $l_+=v_d\tau_+$ is comparable to the positron diffusion length, which is approximately 2500 Å in Si, implying that the electric fields of the order of 10^3 V/cm are sufficient to seriously influence the positron motion. Such electric field strengths are common in the space-charge region of semiconductor surfaces in the presence of surface electron states.

Positron motion is well described in terms of the drift-diffusion approximation similar to the classical carrier transport models. At 300 K we find the positron mobility $\mu_+=120\pm10$ cm^2/V s. In the case of the lowest applied electric fields, the drift velocity is much smaller than the thermal-equilibrium velocity 1.1×10^7 cm/s at 300 K. In this linear-response regime the positron drift velocity depends on the electric field as $\mathbf{v}_d=\mu_+\mathcal{E}$, and consequently the value $\mu_+=120$ cm^2/V s represents the Ohmic mobility of positrons in Si. The Einstein relation yields the positron diffusion coefficient $D_+=3.0\pm0.25$ cm^2/s.

In electron and hole transport the Ohmic region is reached at 300 K when the drift velocity is less than 2×10^6 cm/s (Refs. 5 and 6). The average field in the depletion region of the surface-barrier diode varies from 4.5×10^3 to 1.6×10^4 V/cm with the applied bias voltage V_b extending from $+0.18$ to -4.0 V. The maximum field strength is 3.2×10^4 V/cm corresponding to the positron drift velocity $v_d\leq3.5\times10^6$ cm/s. In this region positron mobility shows no apparent dependence on the applied electric field.

In the high-purity FZ Si sample the positron diffusion coefficient $D_+=3.10\pm0.20$ cm^2/s was found assuming there is no electric field, in close agreement with the value calculated from the positron mobility through the Einstein relation. This supports the fact that in this sample the influence of the electric field on positron motion is

small, although the actual field strength is not known.

Mills and Pfeiffer[4] have measured the positron drift velocities in Si crystals in the form of a lithium compensated silicon γ-ray detector by observing the Doppler shift of the annihilation line. They found the positron mobilities $\mu_+ = 460 \pm 20$ and 173 ± 15 cm^2/V s at 80 and 184 K, respectively. Comparison between these results cannot be done directly because of the different temperatures. If the low-temperature values are extrapolated to 300 K assuming μ_+ to follow the $T^{-3/2}$-law characteristic of positron scattering from acoustic phonons, though the mobilities quoted above suggest a weaker temperature dependence, we find μ_+ to be from 65 to 80 cm^2/V s. This is in reasonable agreement with the positron mobility of 120 cm^2/V s found here, in particular as the exact temperature dependence is not known.

Simpson *et al.*[14] have recently published a measurement of the positron mobility in Si using a ^{22}Na source and the positron-lifetime technique. Their work relies upon the drift of positrons to a Au-Si interface, after implantation through the Au overlayer to Si, and measurement of the intensity of the lifetime component originating from annihilation at the interface. They give the positron mobilities 100 ± 18 and 990 ± 170 cm^2/V s at 295 and 104 K, respectively. The 295 K mobility is in good accord with the present value of 120 ± 10 cm^2/V s.

The positron diffusion coefficient D_+ or the diffusion length L_+ are often given in terms of the energy E_0 defined as $L_+ = (D_+\tau)^{1/2} = (\alpha/\rho)(E_0/\text{keV})^n$. The positron diffusion coefficient $D_+ = 3.0 \pm 0.25$ cm^2/s yields $E_0 = 5.04 \pm 0.10$ keV and $L_+ = 2570 \pm 100$ Å. In the pure Si sample the energy E_0 is 5.10 ± 0.10 keV assuming zero electric field. These values agree with $E_0 = 4.90$ keV calculated from the diffusion coefficient $D_+ = 2.7 \pm 0.2$ cm^2/s reported by Schultz *et al.*[12] for floating zone-refined Si.

The lattice-scattering mechanisms for positrons in Si are predominantly due to acoustic and nonpolar optical phonons. Simple estimates of scattering rates indicate that the possibility of scattering from electrons and at 300 K also from neutral or ionized impurities is vanishingly small compared to phonon scattering.[11] Boev *et al.*[32] have calculated the positron deformation potential $E_d = -6.19$ eV in Si. In the deformation potential approach this yields the diffusion coefficient $D_+ = 3.05$ cm^2/s at 300 K for positron scattering from longitudinal acoustic phonons. This value for the diffusion coefficient assumes the effective positron mass $1.5m_e$. Though there is some uncertainty in the effective mass, comparison with the diffusion coefficient of 3.0 ± 0.25 cm^2/s asserts that the lattice scattering is largely due to positron coupling to longitudinal acoustic phonons. It is also apparent that a weak coupling to phonons gives a good description of positron motion in Si at 300 K.

The temperature dependencies of positron mobility deduced from the works of Mills and Pfeiffer[4] and of Simpson *et al.*[14] are different from each other and also different from that expected for simple acoustic-phonon scattering. The former gives a weaker temperature dependence, the latter clearly stronger, although the values reported using the Doppler, lifetime, and also the low-energy positron beam techniques in this work are in good agreement at 300 K. This discrepancy remains unclear.

In conclusion, the measurement of positron motion in the space-charge region of a Au-Si surface-barrier diode demonstrates the influence of electric field on positron transport. An electric field of the order of 10 kV/cm gives rise to a drift length between 2 and 3 μm. Within the drift-diffusion approximation similar to the classical carrier transport models, we find the Ohmic positron mobility of 120 ± 10 cm^2/V s at 300 K. The positron diffusion coefficient is 3.0 ± 0.25 cm^2/s. Comparing with theoretical calculations of positron-phonon interaction we can attribute positron scattering mainly to coupling with longitudinal acoustic phonons at 300 K.

---

*Permanent address: Centre d'Etudes Nucléaires de Saclay, Institut National des Sciences et Techniques Nucléaires, 91191 Gif sur Yvette, France.

[1] P. J. Schultz and K. G. Lynn, Rev. Mod. Phys. **60**, 701 (1988).
[2] E. Soininen, H. Huomo, P. A. Huttunen, J. Mäkinen, A. Vehanen, and P. Hautojärvi, Phys. Rev. B **41**, 6227 (1990).
[3] A. P. Mills, Jr. and L. Pfeiffer, Phys. Rev. Lett. **36**, 1389 (1976).
[4] A. P. Mills, Jr. and L. Pfeiffer, Phys. Lett. **63A**, 118 (1977).
[5] C. Canali, C. Jacoboni, F. Nava, G. Ottaviani, and A. Alberigi-Quaranta, Phys. Rev. B **12**, 2265 (1975).
[6] G. Ottaviani, L. Reggiani, C. Canali, F. Nava, and A. Alberigi-Quaranta, Phys. Rev. B **12**, 3318 (1975).
[7] L. Reggiani, C. Canali, F. Nava, and G. Ottaviani, Phys. Rev. B **16**, 2781 (1977).
[8] C. Jacoboni, F. Nava, C. Canali, and G. Ottaviani, Phys. Rev. B **24**, 1014 (1981).
[9] B. Nielsen, K. G. Lynn, A. Vehanen, and P. J. Schultz, Phys. Rev. B **32**, 2296 (1985).
[10] H. H. Jorch, K. G. Lynn, and I. K. MacKenzie, Phys. Rev. Lett. **47**, 362 (1981).
[11] H. H. Jorch, K. G. Lynn, and T. McMullen, Phys. Rev. B **30**, 93 (1984).
[12] P. J. Schultz, E. Tandberg, B. Nielsen, T. E. Jackman, M. W. Denhoff, and G. C. Aers, Phys. Rev. Lett. **61**, 187 (1988).
[13] A. Uenodo, S. Tanigava, and Y. Ohji, in *Positron Annihilation*, edited by L. Dorikens-Vanpraet, M. Dorikens, and D. Segers (World Scientific, Singapore, 1989), p. 711.
[14] R. I. Simpson, M. G. Stewart, C. D. Beling, and M. Charlton, J. Phys. Condens. Matter **1**, 7251 (1989).
[15] C. Corbel, P. Hautojärvi, J. Mäkinen, A. Vehanen, and D. Mathiot, J. Phys. Condens. Matter **1**, 6315 (1989).
[16] H. Huomo, E. Soininen, and A. Vehanen, Appl. Phys. A **49**, 647 (1989).
[17] A. Perkins and P. J. Carbotte, Phys. Rev. B **1**, 101 (1970).
[18] P. Kubica and A. T. Stewart, Phys. Rev. Lett. **34**, 852 (1975).
[19] M. A. Shulman, G. M. Beardsley, and S. Berko, Appl. Phys. **5**, 367 (1975).
[20] K. Saarinen, P. Hautojärvi, A. Vehanen, R. Krause, and G. Dlubek, Phys. Rev. B **39**, 5287 (1989).
[21] M. Puska, C. Corbel, and R. M. Nieminen, Phys. Rev. B **41**,

9980 (1990).

[22]J. Mäkinen, C. Corbel, P. Hautojärvi, P. Moser, and F. Pierre, Phys. Rev. B **39**, 10 162 (1989).

[23]M. A. Green, Solid-State Electron. **19**, 421 (1976).

[24]J. Lahtinen, A. Vehanen, H. Huomo, J. Mäkinen, P. Huttunen, K. Rytsölä, M. Bentzon, P. Hautojärvi, Nucl. Instrum. Methods B **17**, 73 (1986).

[25]T. McMullen, in *Positron Annihilation,* edited by P. C. Jain, R. M. Singru, and K. P. Copinathan (World Scientific, Singapore, 1985), p. 657.

[26]R. M. Nieminen and J. Oliva, Phys. Rev. B **22**, 2226 (1980).

[27]H. K. Henisch, *Semiconductor Contacts* (Clarendon, Oxford, 1984).

[28]S. Valkealahti and R. M. Nieminen, Appl. Phys. A **32**, 95 (1983); **35**, 51 (1984).

[29]A. Vehanen, K. Saarinen, P. Hautojärvi, and H. Huomo, Phys. Rev. B **35**, 4606 (1987).

[30]S. Dannefaer, Phys. Status Solidi A **102**, 481 (1987).

[31]H. Huomo, A. Vehanen, M. D. Bentzon, and P. Hautojärvi, Phys. Rev. B **35**, 8252 (1987).

[32]O. V. Boev, M. J. Puska, and R. M. Nieminen, Phys. Rev. B **36**, 7786 (1987).